Title

CdiA from Enterobacter cloacae Delivers a Toxic Ribosomal RNase into Target Bacteria

Journal

Structure, 22(5)

ISSN

1359-0278

Authors

Beck, Christina M
Morse, Robert P
Cunningham, David A
et al.

Publication Date

2014-05-01

DOI

10.1016/j.str.2014.02.012

Peer reviewed

Published in final edited form as:
Structure. 2014 May 6; 22(5): 707–718. doi:10.1016/j.str.2014.02.012.

CdiA from *Enterobacter cloacae* delivers a toxic ribosomal RNase into target bacteria

Christina M. Beck[1,†], **Robert P. Morse**[2,†], **David A. Cunningham**[1], **Angelina Iniguez**[2], **David A. Low**[1,3], **Celia W. Goulding**[2,4], and **Christopher S. Hayes**[1,3,*]

[1]Department of Molecular, Cellular and Developmental Biology, University of California, Santa Barbara, Santa Barbara, CA 93106-9625, USA

[2]Department of Molecular Biology and Biochemistry, University of California, Irvine, Irvine, CA 92697, USA

[3]Biomolecular Science and Engineering Program, University of California, Santa Barbara, Santa Barbara, CA 93106-9625, USA

[4]Department of Pharmaceutical Sciences, University of California, Irvine, Irvine, CA 92697, USA

Summary

Contact-dependent growth inhibition (CDI) is one mechanism of inter-bacterial competition. CDI$^+$ cells export large CdiA effector proteins, which carry a variety of C-terminal toxin domains (CdiA-CT). CdiA-CT toxins are specifically neutralized by cognate CdiI immunity proteins to protect toxin-producing cells from auto-inhibition. Here, we use structure determination to elucidate the activity of a unique CDI toxin from *Enterobacter cloacae* (ECL). The structure of CdiA-CT^{ECL} resembles the C-terminal nuclease domain of colicin E3, which cleaves 16S ribosomal RNA to disrupt protein synthesis. In accord with this structural homology, we show that CdiA-CT^{ECL} uses the same nuclease activity to inhibit bacterial growth. Surprisingly, although colicin E3 and CdiA^{ECL} carry equivalent toxin domains, the corresponding immunity proteins are unrelated in sequence, structure and toxin-binding site. Together, these findings reveal unexpected diversity amongst 16S rRNases and suggest that these nucleases are robust and versatile payloads for a variety of toxin-delivery platforms.

Introduction

Bacterial genomes and plasmids encode a variety of peptide and protein toxins that mediate inter-bacterial competition. Colicins were the first of such toxins to be identified and characterized from strains of *Escherichia coli*. Subsequently, it was discovered that other bacteria release similar toxins, which are now collectively termed bacteriocins (Cascales et

*Corresponding author. Ph: (805) 893-2028, chayes@lifesci.ucsb.edu.
†These authors contributed equally to this study.

al., 2007). Bacteriocins are diffusible proteins that parasitize cell-envelope proteins to enter and kill bacteria. These toxins are composed of three domains, each responsible for a distinct step in the cell-killing pathway. The central domain binds specific receptors on the surface of susceptible bacteria. The N-terminal domain mediates translocation across the cell envelope, and the C-terminal domain carries the bacteriocidal activity. This modular structure allows for delivery of diverse C-terminal toxins using conserved translocation and receptor-binding domains. For example, colicins E2 through E9 share virtually identical N-terminal domains but carry different C-terminal toxins with DNase (Schaller and Nomura, 1976), ribosomal RNase (Bowman et al., 1971; Senior and Holland, 1971) or tRNA anticodon nuclease activities (Ogawa et al., 1999). Bacteriocin genes are always closely linked to immunity genes, which encode small proteins that specifically bind and neutralize the toxin domains. Thus, cells that harbor bacteriocinogenic plasmids are protected from toxin activity, but they may still be susceptible to the bacteriocins produced from other plasmids. Many different bacteriocin/immunity types are typically present in a given environment (Gordon et al., 1998; Riley and Gordon, 1992), and these plasmids are predicted to have a significant impact on bacterial population structures (Chao and Levin, 1981; Czaran et al., 2002).

Research over the past decade has uncovered additional bacterial competition systems that require direct cell-to-cell contact for toxin delivery (Aoki et al., 2010; Aoki et al., 2005; Hood et al., 2010; MacIntyre et al., 2010; Zheng et al., 2011). There are at least two pathways – mediated by type V and type VI secretion systems – for contact-dependent toxin delivery between Gram-negative bacteria (Ruhe et al., 2013a; Silverman et al., 2012). The type V mechanism was the first identified and this phenomenon was termed "CDI" for contact-dependent growth *i*nhibition (Aoki et al., 2005). CDI is mediated by the CdiB/CdiA family of two-partner secretion proteins. CdiB is a predicted β-barrel protein that resides in the outer membrane and is required for export of CdiA effectors. CdiA proteins are very large (250 – 600 kDa) and are thought to extend from the inhibitor cell to interact with neighboring target bacteria. Although CdiA and bacteriocins are unrelated, these effector proteins share a number of general features. Like bacteriocins, CdiA proteins bind to specific receptors on the surface of target bacteria and these interactions determine the target-cell range (Aoki et al., 2008; Ruhe et al., 2013b). Additionally, CDI toxin activity is carried at the extreme C-terminus of CdiA, and some portion of this CdiA-CT region is translocated into target bacteria (Aoki et al., 2010; Morse et al., 2012; Webb et al., 2013). CDI loci also encode CdiI immunity proteins, which bind and inactivate CdiA-CTs to protect toxin-producing cells from auto-inhibition. Finally, CDI systems deploy a variety of toxin domains with distinct biochemical activities. Remarkably, chimeric CDI effectors can be produced by fusing different toxins onto CdiA at the conserved VENN peptide motif that demarcates the CdiA-CT region (Aoki et al., 2010). There is also evidence that bacteria exchange *cdiA-CT/cdiI* genes through horizontal transfer (Poole et al., 2011), suggesting that effector modularity is exploited to switch toxin/immunity type. In fact, bacteria collectively contain a large repository of toxin/immunity genes that are shared by a variety of toxin-delivery systems (Holberger et al., 2012; Poole et al., 2011; Zhang et al., 2012; Zhang et al., 2011). For example, at least two CdiA proteins carry toxins with homology to bacteriocin nucleases. $CdiA^{Dd3937}$ from *Dickeya dadantii* 3937 carries a CT domain with 35% identity

to the pyocin S3 DNase domain (Aoki et al., 2010), and the C-terminal region of CdiA^{K96243} from *Burkholderia pseudomallei* K96243 is 49% identical to the anticodon tRNase domain of colicin E5. Biochemical analyses have confirmed that each of these CDI toxins has the same nuclease activity as the corresponding bacteriocin (Aoki et al., 2010; Nikolakakis et al., 2012). Together, these observations suggest that CDI loci integrate toxin/immunity gene pairs from diverse sources and that this diversity contributes to interstrain competition.

In an effort to understand CDI toxin/immunity diversity and uncover new toxin activities, we have initiated structural studies of CdiA-CT/CdiI pairs from various bacteria. Here, we describe the structure and function of the CDI toxin/immunity protein pair from *Enterobacter cloacae* ATCC 13047 (ECL). The CdiA-CT^{ECL} toxin shares no significant sequence identity with proteins of known function, but the three-dimensional structure of CdiA-CT^{ECL} reveals similarity to the C-terminal nuclease domain of colicin E3. In accord with the structural homology, CdiA-CT^{ECL} cleaves 16S rRNA at the same site as colicin E3 and this nuclease activity is responsible for growth inhibition. By contrast, CdiI^{ECL} does not resemble the colicin E3 immunity protein (ImE3), and the two immunity proteins bind to different sites on their respective cognate toxin domains. Inspection of other CdiA proteins from *Erwinia chrysanthemi* EC16 (Uniprot: P94772), *Enterobacter hormaechei* ATCC 49162 (F5S237) and *Pseudomonas viridiflava* UASWS0038 (K6CF79) has revealed that their toxin domains share a common nuclease motif with colicin E3 (Walker et al., 2004). Analysis of CdiA-CT^{EC16} from *Erwinia chrysanthemi* EC16 confirms that this toxin has 16S rRNase activity and demonstrates that the associated CdiI^{EC16} immunity protein is specific to CdiA-CT^{EC16} and does not provide protection against the CdiA-CT^{ECL} nuclease. Together, these observations indicate that 16S rRNase toxins are more diverse and widespread than previously recognized.

Results

Crystallization and structure of the CdiA-CT^{ECL}/CdiI^{ECL} complex

In a previous study, we used structural analysis to determine the activities of CDI toxins from *E. coli* EC869 and *Burkholderia pseudomallei* 1026b (Morse et al., 2012). Because the CDI toxin/immunity pair from *E. cloacae* ATCC 13047 shares no sequence homology with proteins of known function, we followed a similar structure-based approach to characterize this system. The CdiA-CT^{ECL} region is demarcated by the AENN peptide motif and corresponds to residues Ala3087 to Asp3321 of full-length CdiA^{ECL}. We co-expressed CdiA-CT^{ECL} with His$_6$-tagged CdiI^{ECL} and purified the complex to near homogeneity (Fig. S1A). The N-terminal region of CdiA-CT^{ECL} was partially degraded during crystallization (Fig. S1A), presumably because this region is disordered. Similar N-terminal degradation has been observed with other CdiA-CTs (Morse et al., 2012). The CdiA-CT^{ECL}/CdiI^{ECL} complex crystallized in space group P4$_1$22 with one heterodimeric complex per asymmetric unit (Fig. S1B). The structure was solved by selenium multiple wavelength anomalous dispersion (Se-MAD) phasing to 2.4 Å resolution. The final refined model contains CdiA-CT^{ECL} residues 160 – 235 (numbered from Ala1 of the AENN motif) and CdiI^{ECL} residues

1 – 145. In addition, 62 well-resolved water molecules are included in the final model resulting in R_{work}/R_{free} of 18.3/23.7 (Table 1).

The resolved C-terminal domain of CdiA-CT^{ECL} consists of an N-terminal α-helix followed by a twisted five-stranded antiparallel β-sheet (Fig. 1A). The domain contains two long loops, L2 and L4, which connect β1 to β2 and β3 to β4, respectively (Fig. 1A). Weak electron density was observed for loop L4, likely due to its flexibility, and thus Ser206 – Asn211 were modeled as alanine residues. The CdiI^{ECL} immunity protein comprises three- and four-stranded antiparallel β-sheets, forming a β-sandwich that is decorated with three α-helices (Fig. 1A). The toxin and immunity protein interface is elaborate and mediated by a series of hydrogen-bonds (H-bond), electrostatic and hydrophobic interactions (Fig. 1B & Table S1). CdiA-CT^{ECL} residues within loops L2 – L6 form H-bonds and ion-pair interactions with CdiI^{ECL} residues in loops L1′, L2′ and L3′ and the edge of the β-sandwich (β3′, β5′ and β6′) (Fig. 1B). A water-mediated network of H-bonds also contributes to the interface, resulting in more than 20 ion-pair/H-bond interactions between toxin and immunity proteins (Fig. 1B & Table S1). In addition, there is a hydrophobic interface of approximately 300 Å^2 consisting of Ile178, Val192, Tyr199 and Phe216 from CdiA-CT^{ECL}, and Phe76, Phe78, Val95 and Phe97 from CdiI^{ECL} (Fig. 1C). Overall, the CdiA-CT^{ECL}/CdiI^{ECL} complex has an interface of 1399 Å^2, burying 27.6 and 17.1% of the solvent-accessible surface areas of the toxin and immunity proteins, respectively.

CdiA-CT^{ECL} is structurally homologous to the nuclease domain of colicin E3

CdiA-CT^{ECL} shares no structural homology with previously characterized CDI toxins from *E. coli* EC869 and *B. pseudomallei* 1026b (Morse et al., 2012; Nikolakakis et al., 2012). Searches for structural homologues using the DALI server (Holm and Rosenstrom, 2010) revealed that CdiA-CT^{ECL} is similar to the C-terminal nuclease domain of colicin E3 (ColE3-CT). Colicin E3 is a plasmid-encoded bacteriocin found in some *E. coli* strains, and its nuclease domain cleaves 16S rRNA between residues A1493 and G1494 (*E. coli* numbering) to interfere with protein synthesis (Lancaster et al., 2008; Ng et al., 2010). The CdiA-CT^{ECL} and ColE3-CT domains share a twisted antiparallel β-sheet and superimpose with an rmsd of 2.1 Å over 76 α-carbons, corresponding to a Z-score of 4.8, whereas the sequence identity between the two domains is approximately 18% (Figs. 2A & S2A). Residues Asp510, His513 and Glu517 of colicin E3 are thought to function directly in catalysis (Ng et al., 2010; Soelaiman et al., 2001; Walker et al., 2004), and CdiA-CT^{ECL} residues Asp203, Asp205 and Lys214 superimpose upon these colicin E3 active site residues (Figs. 2B & S2A). Together, these structural similarities suggest that CdiA-CT^{ECL} may share 16S rRNA nuclease activity with colicin E3.

Although the CdiA-CT^{ECL} and ColE3-CT toxin domains are structurally similar, the corresponding immunity proteins are not related to one another in either primary or tertiary structure (Figs. S3A & S3B). The colicin E3 immunity protein (ImE3) is significantly smaller than CdiI^{ECL} (~9.9 versus 16.9 kDa), and the two proteins have different folds (Fig. S3B). A DALI search reveals that CdiI^{ECL} is most similar to the Whirly family of single-stranded DNA binding proteins (Desveaux et al., 2005). The closest structural homologues are two proteins of unknown function from cyanobacteria (PDB ID codes: 2IT9 and 2NVN),

which superimpose onto CdiI^{ECL} with rmsd of 3.6 – 4.0 Å over 120 – 122 α-carbons (Fig. S3C). CdiI^{ECL} and ImE3 also bind their cognate toxins differently. ImE3 binds to an 'exosite' that leaves the colicin E3 active site exposed (Carr et al., 2000), whereas CdiI^{ECL} binds directly over the predicted active site (Fig. 2C). Structural alignment of the complexes shows that immunity protein binding occurs at distinct non-overlapping positions (Fig. 2D). Interestingly, ColE3-CT contains a C-terminal extension not found in CdiA-CT^{ECL} (Fig. 2A). This C-terminal tail forms a short α-helix in one ColE3-CT structure (Soelaiman et al., 2001), and this element would likely interfere with CdiI^{ECL} binding were it present in CdiA-CT^{ECL}. Similarly, the orientation of loop L2 differs considerably between the toxins (Fig. 2A), and these loops could block the binding of non-cognate immunity proteins (Fig. 2D). Despite these differences, each immunity protein is predicted to prevent its cognate toxin from entering the ribosome A site (Figs. S4) (Ng et al., 2010), and therefore toxin inactivation is fundamentally the same for both systems.

CdiA-CT^{ECL} cleaves 16S rRNA in vivo to inhibit cell growth

The structural resemblance of CdiA-CT^{ECL} to ColE3-CT suggests that the CDI toxin also cleaves 16S rRNA. To test this prediction, we cloned *cdiA-CT*^{ECL} under the control of an arabinose-inducible promoter and asked whether 16S rRNA is cleaved upon induction with L-arabinose. *E. coli* cells carrying the *cdiA-CT*^{ECL} construct do not grow when the media is supplemented with L-arabinose (Fig. 3A), confirming that CdiA-CT^{ECL} is an inhibitory toxin. We isolated total RNA from the inhibited cells and analyzed 16S rRNA by northern blot. This analysis revealed that 16S rRNA is cleaved in cells expressing *cdiA-CT*^{ECL}, but remains intact in control cells that carry the vector plasmid alone (Fig. 3B). We next tested CdiI^{ECL} function to determine whether it neutralizes the growth inhibition and nuclease activities of CdiA-CT^{ECL}. We cloned *cdiI*^{ECL} under the control of an IPTG-inducible promoter and introduced the resulting plasmid into cells that harbor the arabinose-inducible *cdiA-CT*^{ECL} construct. Cells expressing both *cdiA-CT*^{ECL} and *cdiI*^{ECL} grow at the same rate as control cells that carry empty vector plasmids (Fig. 3A), indicating that CdiI^{ECL} prevents CdiA-CT^{ECL}-mediated growth inhibition. Furthermore, northern analysis shows that 16S rRNA is not cleaved in cells that co-express *cdiA-CT*^{ECL} and *cdiI*^{ECL} (Fig. 3B), demonstrating that the immunity protein also blocks nuclease activity. Together, these results show that CdiA-CT^{ECL} and CdiI^{ECL} constitute a cognate toxin/immunity pair that targets the ribosome.

CdiI^{ECL} immunity function is specific for its cognate toxin

At least one other CdiA protein is predicted to possess 16S rRNase activity. Kleanthous and colleagues discovered that HecA from *Erwinia chrysanthemi* EC16 contains the same catalytic motif as colicin E3 (Fig. S2B) (Walker et al., 2004). HecA was originally identified as an adhesin that promotes bacterial colonization of plant hosts (Rojas et al., 2002; Rojas et al., 2004), but this protein shares 68% sequence identity with a known CdiA effector (Uniprot: E0SCQ6) from *Dickeya dadantii* 3937 (Aoki et al., 2010). Together, these observations suggest that HecA actually functions in CDI, and therefore we refer to this protein as CdiA^{EC16}. To test toxin activity, we cloned the *cdiA-CT*^{EC16} sequence under control of an arabinose-inducible promoter for expression in *E. coli* cells. As predicted, cell growth is inhibited when *cdiA-CT*^{EC16} expression is induced (Fig. 3C), and northern

analysis shows that 16S rRNA cleavage in the inhibited cells (Fig. 3D). Because CDI systems are always arranged as toxin/immunity gene pairs, we tested the small open reading frame found immediately downstream of *cdiA*^{EC16} for immunity function. The predicted *cdiI*^{EC16} gene blocks the growth inhibition and nuclease activities associated with *cdiA-CT*^{EC16} expression (Figs. 3C & 3D). CdiA-CT^{EC16} and CdiI^{EC16} do not share significant sequence identity with the toxin/immunity proteins from *E. cloacae* (Fig. S2 and not shown), suggesting that each immunity protein is specific for its cognate toxin. Indeed, we found that *cdiI*^{ECL} and *cdiI*^{EC16} only protect cells from the inhibitory effects of their corresponding toxins (Figs. 3A & 3C). Similarly, each immunity gene specifically blocks the nuclease activity associated with its cognate toxin (Figs. 3B & 3D). Thus, although CdiA-CT^{ECL} and CdiA-CT^{EC16} share a common growth inhibition activity, the associated immunity proteins only provide protection against their cognate toxins.

Purified CdiA-CT^{ECL} and CdiA-CT^{EC16} cleave 16S rRNA in vitro

In principle, CdiA-CT^{ECL} and CdiA-CT^{EC16} could induce an endogenous nuclease activity that actually catalyzes 16S rRNA cleavage. Therefore, we tested purified toxins for nuclease activity *in vitro*. Each CdiA-CT/CdiI-His$_6$ pair was first purified as a complex. Toxins were then eluted away from immunity proteins using Ni^{2+}-affinity chromatography under denaturing conditions. Purified toxins were refolded by dialysis against non-denaturing buffer prior to activity assays. Before testing nuclease activity, we first confirmed that each refolded CdiA-CT is able to re-bind its cognate immunity protein. We mixed CdiI-His$_6$ with either cognate or non-cognate toxin and subjected the mixtures to Ni^{2+}-affinity chromatography under non-denaturing conditions. Each CdiA-CT co-purified with its cognate immunity protein (Fig. 4A), indicating that the toxins can re-establish specific binding interactions after denaturation and refolding. We next treated ribosomes with purified toxins and analyzed the reactions by northern blot hybridization. Both CdiA-CT^{ECL} and CdiA-CT^{EC16} cleave a 3′-fragment from 16S rRNA, and the activity of each toxin is effectively blocked by equimolar cognate CdiI protein (Fig. 4B). These results indicate that each toxin is directly responsible for 16S rRNA cleavage.

We next used primer extension to determine whether the CDI toxins cleave 16S rRNA at the same position as colicin E3. We generated an oligonucleotide that hybridizes to residues C1501 – C1521 of *E. coli* 16S rRNA (Fig. 5A) and used it as a primer in reverse transcription reactions to screen for cleavage sites. Residue U1498 of 16S rRNA is methylated at the N3 position (Fig. 5A) and this modified base is predicted to interfere with reverse transcription. Therefore, we repeated the *in vitro* nuclease reactions using ribosomes isolated from an *E. coli* Δ*rsmE::kan* mutant, which lacks the U1498 methyltransferase (Basturea et al., 2006). Analysis of these nuclease reactions shows a strong primer-extension arrest corresponding to residue G1494 (Figs. 5A & 5B). This primer extension product is not observed when ribosomes are mock-treated with buffer, nor when the reactions contain equimolar cognate CdiI protein (Fig. 5B). These data are consistent with CdiA-CT-mediated cleavage of the phosphodiester bond linking residues A1493 and G1494 (Fig. 5A). Thus, CdiA-CT^{ECL} and CdiA-CT^{EC16} both appear to cleave 16S rRNA at the same site as colicin E3.

Mutational analysis confirms active site residues identified in the CdiA-CT^{ECL} structure

The side-chains of CdiA-CT^{ECL} Asp203 and Lys214 overlay with active site residues Asp510 and Glu517 (respectively) of colicin E3 (Figs. 2B & S2A). However, because loop L4 is not well resolved in the CdiA-CT^{ECL} structure, it is difficult to unambiguously identify a catalytic residue corresponding to His513 of colicin E3. Therefore, we mutated CdiA-CT^{ECL} residues Asp203, Asp205, His207 and Lys214 individually to alanine and tested the resulting proteins for toxicity *in vivo* and 16S rRNase activity *in vitro*. CdiA-CT^{ECL} variants containing Asp203Ala, His207Ala or Lys214Ala mutations have no effect on *E. coli* cell growth (Fig. 6A), suggesting that nuclease activity is disrupted. The Asp205Ala variant shows a delayed inhibition phenotype, in which cell growth arrests ~90 min after toxin expression is induced (Fig. 6A). Comparable results were obtained with *in vitro* reactions using purified toxin variants. CdiA-CT^{ECL} carrying the Asp203Ala, His207Ala and Lys214Ala mutations have no detectable rRNase activities *in vitro*, whereas the Asp205Ala variant exhibits lower activity than the wild-type enzyme (Fig. 6B). We note that all CdiA-CT^{ECL} variants appear to be folded properly, because each protein efficiently re-binds cognate CdiI^{ECL} immunity protein *in vitro* (Fig. 6C). Together, these experiments indicate that Asp203, His207 and Lys214 are required for toxin activity and could function in catalysis, whereas Asp205 plays an important yet non-essential role.

CdiA-CT^{ECL} is delivered into target bacteria during CDI

We next asked whether the *E. cloacae* CDI system is expressed and deployed for competition. We reasoned that *E. cloacae* mutants lacking the immunity gene should be susceptible to inhibition. We deleted the *cdiA*^{ECL} and *cdiI*^{ECL} genes and tested the resulting double-mutant strain in competition co-cultures with wild-type *E. cloacae* cells. We found that the *E. cloacae* Δ*cdiA*^{ECL} Δ*cdiI*^{ECL} mutants are not inhibited by wild-type cells in either liquid or solid media (Fig. 7A, grey bars; and data not shown), suggesting that the CDI^{ECL} system is not functional or may not be expressed under laboratory conditions. Therefore, we introduced the *E. coli araBAD* promoter upstream of the *E. cloacae cdi* locus to allow inducible expression and used this inhibitor strain for competitions on solid growth media. When the CDI^{ECL} system is induced, the growth of target cells is suppressed approximately 20-fold compared to co-cultures with *E. cloacae* cells carrying the wild-type *cdi* locus (Fig. 7A, compare white to grey bars). Moreover, target cell growth is restored if they carry a plasmid-borne copy of the *cdiI*^{ECL} immunity gene, but the non-cognate *cdiI*^{EC16} gene provides no protection (Fig. 7A). We also tested the inducible *E. cloacae* inhibitor cells in co-cultures with *E. coli* target cells. Because *E. cloacae* ATCC 13047 uses one of its type VI secretion systems to inhibit *E. coli* (Ruhe et al., 2013b), we first deleted the *tssM1* gene (ECL_01536) from the *E. cloacae* inhibitor strain to inactivate type VI secretion. Remarkably, *E. coli* cells are more sensitive to growth inhibition, with viable target cell counts reduced ~100-fold after four hrs of co-culture (Fig. 7B). Notably, *E. coli* cell growth is unaffected during co-culture with *E. cloacae* containing the wild-type *cdi* locus (Fig. 7B), again indicating that the CDI^{ECL} system is not expressed on lab media. Moreover, *E. coli* targets are protected by plasmid-borne *cdiI*^{ECL}, but not *cdiI*^{EC16} (Fig. 7B), confirming that growth inhibition is due to CdiA-CT^{ECL} toxin activity.

Many CdiA-CT toxins are modular and can be exchanged between different CdiA proteins to generate functional effector molecules (Aoki et al., 2010; Morse et al., 2012; Nikolakakis et al., 2012; Webb et al., 2013). To test whether the CdiA-CT/CdiI^{ECL} toxin/immunity protein complex is functional in the context of another CDI system, we replaced the *cdiA-CT/cdiI*^{EC93} region of the *E. coli* EC93 CDI system with the *E. cloacae* toxin/immunity coding sequences. This fusion produces a chimeric CdiA protein with CdiA-CT^{ECL} grafted onto CdiA^{EC93} at the VENN peptide motif. *E. coli* cells expressing the *cdiA*^{EC93}*-CT*^{ECL} chimera are potent inhibitors, capable of reducing viable *E. coli* target cells ~10^4-fold after three hrs of co-culture (Fig. 8A). Again, target cells that carry the *cdiI*^{ECL} immunity gene are not inhibited and grow to the same level as cells cultured with mock-inhibitor cells that lack a CDI system (Fig. 8A). However, target cells expressing non-cognate *cdiI*^{EC16} are inhibited to the same extent as cells that carry no immunity gene (Fig. 8A). Because the inhibition effect is so profound in these co-culture experiments, we asked whether toxin-damaged ribosomes could be detected in the target cells. We isolated total RNA from each competition co-culture and performed northern blot analysis to assay for RNase activity. Cleaved 16S rRNA is readily detected when the target cells lack immunity or express non-cognate *cdiI*^{EC16} immunity, but this nuclease activity is not observed when target cells carry the cognate *cdiI*^{ECL} gene (Fig. 8B). We also generated and tested inhibitor cells that express chimeric *cdiA*^{EC93}*-CT*^{ECL} containing the His207Ala active-site mutation. Cells expressing the mutant effector do not inhibit *E. coli* targets, and no 16S rRNA cleavage is detected in the competition co-culture (Figs. 8A & 8B). Together, these results demonstrate that the CdiA-CT^{ECL} toxin is delivered into target bacteria during CDI and that 16S RNase activity is solely responsible for growth inhibition.

Discussion

CdiA proteins carry a variety of sequence-diverse C-terminal domains, which represent a collection of distinct toxins. Determining the biochemical activities of so many different toxins remains an important problem in the field (Aoki et al., 2010; Ruhe et al., 2013a). Aravind and colleagues have successfully used comparative sequence analyses to predict that many CdiA-CT toxins have nuclease activities (Zhang et al., 2012). However, these predictions often do not identify specific nucleic acid substrates and may be inaccurate in some instances. In fact, the current annotation for CdiA-CT^{ECL} (Pfam PF15526, http://pfam.sanger.ac.uk/family/Toxin_46) suggests that this toxin adopts a BECR (Barnase-EndoU-colicin E5/RelE) protein fold and targets tRNA molecules for cleavage. The work presented here demonstrates that CdiA-CT^{ECL} is actually most similar to the C-terminal nuclease domain of colicin E3. Consistent with this structural homology, CdiA-CT^{ECL} is a site-specific 16S rRNase rather than a tRNase. Furthermore, we note that even accurate protein-fold predictions can lead to erroneous assignments of biochemical activity. For example, CdiA-CT^{Bp1026b} from *Burkholderia pseudomallei* 1026b has the same fold as type IIS restriction endonucleases, yet this toxin is a specific tRNase and has no detectable DNase activity (Morse et al., 2012; Nikolakakis et al., 2012). These discrepancies between prediction and experimental characterization underscore the need for careful biochemical analysis to test sequence-based hypotheses.

The activity of colicin E3 was first described over 40 years ago (Bowman et al., 1971; Senior and Holland, 1971), yet a catalytic mechanism has only recently been proposed based on the structure of the enzyme bound to the ribosome (Ng et al., 2010). The mechanistic model postulates that Glu517 of colicin E3 acts a general base to abstract a proton from the 2´-OH of 16S rRNA residue A1493. The resulting alkoxide subsequently attacks the phosphodiester linking A1493 and G1494 to cleave the 16S rRNA chain. The side-chain of His513 is thought to stabilize the transition state as well as donate a proton to the 5´-OH leaving group after cleavage. Colicin E3 residues Asp510 and Glu515 are within H-bonding distance of His513 and may promote protonation of its imidazole ring (Ng et al., 2010). Comparative structure analysis suggests that residues Asp203, Asp205 and Lys214 of CdiA-CT^{ECL} are involved in catalysis because they are in the same relative positions as Asp510, His513 and Glu517 (respectively) of colicin E3. The superimposition of these residues is remarkable given that loop L4 of CdiA-CT^{ECL}, which contains the predicted active-site residues, is significantly longer and more flexible than the corresponding region in colicin E3 (see Fig. 2A). Mutagenesis experiments confirm that these CdiA-CT^{ECL} residues are important for nuclease activity, but it is not clear that the two enzymes share the same catalytic mechanism. For example, Lys214 in CdiA-CT^{ECL} is unlikely to function as a generalized base as proposed for Glu517 of ColE3-CT, especially as nearby residues Asp203 and Asp205 within CdiA-CT^{ECL} should favor protonation of Lys214. Lysine residues are often found in the active sites of nucleases and typically function to position the scissile phosphodiester or stabilize pentavalent transition states (Gite et al., 1992; Pingoud and Jeltsch, 2001; Richardson et al., 1990). Therefore, it seems likely that Lys214 serves one of the aforementioned functions, leaving His207 to act as the general base that initiates 16S rRNA cleavage. Though we have no structural information for CdiA-CT^{ECL} bound to the ribosome, the available data suggest that colicin E3 and CdiA-CT^{ECL} probably utilize distinct catalytic strategies.

The lack of sequence identity between CdiA-CT^{ECL} and ColE3-CT also raises questions about how the CDI toxin binds to the ribosome. Ramakrishnan, Kleanthous and their colleagues have shown that ColE3-CT loop L2 makes a number of specific contacts with the ribosome A site (Ng et al., 2010). Residues Arg495 and Gln489 bind the nucleobase and phosphate of 16S rRNA residue A1493, Lys496 interacts with C518, and Lys494 holds G530 in the *syn* conformation through a bridging water molecule (Ng et al., 2010). These toxin residues are highly conserved between colicins E3, E4, E6 and cloacin DF, suggesting that these enzymes all bind the ribosome in the same manner. By contrast, not one of these loop L2 residues is shared with CdiA-CT^{ECL} (see Fig. S2A). In fact, loop L2 of CdiA-CT^{ECL} is significantly displaced compared to ColE3-CT. This displacement may result from the binding of CdiI^{ECL}, which would clash with loop L2 if it were in the ColE3-CT conformation. In the absence of CdiI^{ECL}, it is possible that loop L2 of CdiA-CT^{ECL} adopts the same conformation seen in ColE3-CT, but the sequence divergence suggests that each loop makes distinct contacts with the ribosome. ColE3-CT makes additional contacts with ribosomal protein S12 within the A site. Residues Tyr460 – Tyr464 form an intriguing pseudo-β-sheet interaction with the side-chains from His462, Asp463 and Tyr464 making specific H-bond contacts with S12 (Ng et al., 2010). Unfortunately, the corresponding region of CdiA-CT^{ECL} was degraded during crystallization, precluding a direct comparison

of these structures. But again, the primary sequences in this region share no obvious homology, indicating that the two toxins probably interact with ribosomal protein S12 in distinct manners.

Finally, we note that there are several fundamental differences between CdiI^{ECL} and ImE3 immunity proteins. CdiI^{ECL} and ImE3 differ significantly in molecular mass, share less than 12% sequence identity, and bind to non-overlapping sites on their cognate nuclease domains. Moreover, each immunity protein has a distinct tertiary structure and fold. Structural homology searches reveal that CdiI^{ECL} is most similar to the Whirly family of single-stranded DNA-binding proteins. Although this homology is relatively weak (Z-scores 4.1 to 4.3 and rmsd ~4.0 Å), CdiI^{ECL} shares a characteristic topology with all Whirly proteins (see Fig. S3B). The fact that the immunity proteins for colicin E3 and CdiA-CT^{ECL} toxins are unrelated in both primary sequence and tertiary structure suggests that these toxin-immunity pairs have independent origins. Because cognate toxin/immunity gene pairs are closely linked, they must presumably co-evolve as a unit. This process is thought to involve initial changes in the immunity protein, followed by compensatory mutations in the toxin that restore high-binding affinity between the two proteins (Riley, 1993; Tan and Riley, 1997). In general, there are few constraints to impede the drift of immunity genes, because they need only encode proteins that bind toxins. By contrast, toxins are often enzymes and must retain the ability to bind substrates and catalyze reactions. This model is largely supported by analyses showing that immunity proteins diverge more rapidly than toxins (Ruhe et al., 2013a; Tan and Riley, 1997). Thus, although it is formally possible that ImE3 and CdiI^{ECL} arose from a common ancestor, the differences in immunity protein folds make this model much less likely. Based on this reasoning, we speculate that CdiA-CT^{ECL}/CdiI^{ECL} and ColE3-CT/ImE3 evolved from different lineages, and that the structural and enzymatic similarities between the toxins reflect convergent evolution.

Experimental Procedures

Bacterial strains, plasmids and growth conditions

All bacterial strains and plasmids used in this study are listed in Table S2. Bacteria were grown in LB media or LB-agar with the appropriate antibiotics as described in the supplement. *E. cloacae* genes were deleted using the same protocol as described for *E. coli* (Hayes et al., 2002). DNA sequences located upstream and downstream of target genes were amplified and cloned into plasmid pKAN or pSPM (Koskiniemi et al., 2013) to flank kanamycin- or spectinomycin-resistance cassettes, respectively. The resulting plasmids were linearized by restriction endonuclease digestion and electroporated into *E. cloacae* cells expressing the phage λ Red proteins from plasmid pKOBEG (Perez et al., 2007). The details of all strain and plasmid constructions are provided in the supplement.

Protein purification and crystallography

CdiA-CT/CdiI-His$_6$ complexes were purified and the toxin and immunity proteins isolated from one another as described (Diner et al., 2012; Nikolakakis et al., 2012). The CdiA-CT/CdiI^{ECL} complex was crystallized as described (Goulding and Perry, 2003). Crystals were grown at room temperature by hanging drop-vapor diffusion with a reservoir containing 1.5

M $(NH_4)_2SO_4$, 0.1 M Bis Tris (pH 5.1) and 1% (wt/vol) PEG 3350. The structural model was determined as described (Morse et al., 2012). Nonoptimal detector positioning during data collection necessitated the high-resolution limit of 2.4 Å. All crystallography and refinement statistics are presented in Table 1. Atomic coordinates and structure factors have been deposited in the Protein Data Bank (www.pdb.org) as PDB ID code 4NTQ.

Nuclease assays

Ribosomes were isolated from S30 lysates of *E. coli* as described (Diner and Hayes, 2009) and incubated with purified CdiA-CT toxins and CdiI immunity proteins as described in the supplement. All reactions were analyzed by northern blot using a probe complementary to the 3′-end of *E. coli* 16S rRNA. CdiA-CT cleavage sites were determined using ribosomes from *E. coli* Δ*rsmE* cells. Reactions were quenched with guanidinium isothiocyanate-phenol and rRNA extracted for primer extension analysis as described (Diner and Hayes, 2009)

Growth competitions

E. cloacae inhibitor cells were co-cultured with *E. cloacae* Δ*cdiAI* target cells on LB-agar supplemented with 0.2% L-arabinose. Cells were harvested and enumerated as colony forming units (CFU). Immunity function was evaluated through expression of *cdiI* genes in target cells from plasmid constructs as described in the supplement. Cross-species competitions were performed under the same conditions using *E. coli* target cells. Chimeric EC93-ECL CDI systems were expressed from cosmids in *E. coli* EPI100. Inhibitor cells were co-cultured with target cells in LB media. Samples were taken for enumeration of viable target cells. *E. coli* EPI100 cells carrying cosmid pWEB-TNC were used as mock (CDI^-) inhibitors.

Supplementary Material

Refer to Web version on PubMed Central for supplementary material.

Acknowledgments

This work was supported by the National Institutes of Health through grants R21 AI099687 (C.S.H. and C.W.G.) and U01 GM102318 (D.A.L., C.S.H. and C.W.G). We thank the staff at both the Advanced Light Source (U.S. Department of Energy under Contract No. DE-AC02-05CH11231) at Berkeley National Laboratories and the Stanford Synchrotron Radiation Lightsource (supported in part by P41 GM103393) for their invaluable help in data collection. The funders had no role in study design, data collection and analysis, decision to publish or preparation of the manuscript.

References

Aoki SK, Diner EJ, de Roodenbeke CT, Burgess BR, Poole SJ, Braaten BA, Jones AM, Webb JS, Hayes CS, Cotter PA, et al. A widespread family of polymorphic contact-dependent toxin delivery systems in bacteria. Nature. 2010; 468:439–442. [PubMed: 21085179]

Aoki SK, Malinverni JC, Jacoby K, Thomas B, Pamma R, Trinh BN, Remers S, Webb J, Braaten BA, Silhavy TJ, et al. Contact-dependent growth inhibition requires the essential outer membrane protein BamA (YaeT) as the receptor and the inner membrane transport protein AcrB. Mol Microbiol. 2008; 70:323–340. [PubMed: 18761695]

Aoki SK, Pamma R, Hernday AD, Bickham JE, Braaten BA, Low DA. Contact-dependent inhibition of growth in *Escherichia coli*. Science. 2005; 309:1245–1248. [PubMed: 16109881]

Basturea GN, Rudd KE, Deutscher MP. Identification and characterization of RsmE, the founding member of a new RNA base methyltransferase family. RNA. 2006; 12:426–434. [PubMed: 16431987]

Bowman CM, Dahlberg JE, Ikemura T, Konisky J, Nomura M. Specific inactivation of 16S ribosomal RNA induced by colicin E3 in vivo. Proc Natl Acad Sci U S A. 1971; 68:964–968. [PubMed: 4930244]

Carr S, Walker D, James R, Kleanthous C, Hemmings AM. Inhibition of a ribosome-inactivating ribonuclease: the crystal structure of the cytotoxic domain of colicin E3 in complex with its immunity protein. Structure. 2000; 8:949–960. [PubMed: 10986462]

Cascales E, Buchanan SK, Duche D, Kleanthous C, Lloubes R, Postle K, Riley M, Slatin S, Cavard D. Colicin biology. Microbiol Mol Biol Rev. 2007; 71:158–229. [PubMed: 17347522]

Chao L, Levin BR. Structured habitats and the evolution of anticompetitor toxins in bacteria. Proc Natl Acad Sci U S A. 1981; 78:6324–6328. [PubMed: 7031647]

Czaran TL, Hoekstra RF, Pagie L. Chemical warfare between microbes promotes biodiversity. Proc Natl Acad Sci U S A. 2002; 99:786–790. [PubMed: 11792831]

Desveaux D, Marechal A, Brisson N. Whirly transcription factors: defense gene regulation and beyond. Trends Plant Sci. 2005; 10:95–102. [PubMed: 15708347]

Diner EJ, Beck CM, Webb JS, Low DA, Hayes CS. Identification of a target cell permissive factor required for contact-dependent growth inhibition (CDI). Genes Dev. 2012; 26:515–525. [PubMed: 22333533]

Diner EJ, Hayes CS. Recombineering reveals a diverse collection of ribosomal proteins L4 and L22 that confer resistance to macrolide antibiotics. J Mol Biol. 2009; 386:300–315. [PubMed: 19150357]

Gite S, Reddy G, Shankar V. Active-site characterization of S1 nuclease. I. Affinity purification and influence of amino-group modification. Biochem J. 1992; 285(Pt 2):489–494. [PubMed: 1637340]

Gordon DM, Riley MA, Pinou T. Temporal changes in the frequency of colicinogeny in *Escherichia coli* from house mice. Microbiology. 1998; 144(Pt 8):2233–2240. [PubMed: 9720045]

Goulding CW, Perry LJ. Protein production in *Escherichia coli* for structural studies by X-ray crystallography. J Struct Biol. 2003; 142:133–143. [PubMed: 12718925]

Hayes CS, Bose B, Sauer RT. Proline residues at the C terminus of nascent chains induce SsrA tagging during translation termination. J Biol Chem. 2002; 277:33825–33832. [PubMed: 12105207]

Holberger LE, Garza-Sanchez F, Lamoureux J, Low DA, Hayes CS. A novel family of toxin/antitoxin proteins in *Bacillus* species. FEBS Lett. 2012; 586:132–136. [PubMed: 22200572]

Holm L, Rosenstrom P. Dali server: conservation mapping in 3D. Nucleic Acids Res. 2010; 38:W545–W549. [PubMed: 20457744]

Hood RD, Singh P, Hsu F, Guvener T, Carl MA, Trinidad RR, Silverman JM, Ohlson BB, Hicks KG, Plemel RL, et al. A type VI secretion system of *Pseudomonas aeruginosa* targets a toxin to bacteria. Cell Host Microbe. 2010; 7:25–37. [PubMed: 20114026]

Koskiniemi S, Lamoureux JG, Nikolakakis KC, t'Kint de Roodenbeke C, Kaplan MD, Low DA, Hayes CS. Rhs proteins from diverse bacteria mediate intercellular competition. Proc Natl Acad Sci U S A. 2013; 110:7032–7037. [PubMed: 23572593]

Lancaster LE, Savelsbergh A, Kleanthous C, Wintermeyer W, Rodnina MV. Colicin E3 cleavage of 16S rRNA impairs decoding and accelerates tRNA translocation on *Escherichia coli* ribosomes. Mol Microbiol. 2008; 69:390–401. [PubMed: 18485067]

MacIntyre DL, Miyata ST, Kitaoka M, Pukatzki S. The *Vibrio cholerae* type VI secretion system displays antimicrobial properties. Proc Natl Acad Sci U S A. 2010; 107:19520–19524. [PubMed: 20974937]

Morse RP, Nikolakakis KC, Willett JL, Gerrick E, Low DA, Hayes CS, Goulding CW. Structural basis of toxicity and immunity in contact-dependent growth inhibition (CDI) systems. Proc Natl Acad Sci U S A. 2012; 109:21480–21485. [PubMed: 23236156]

Ng CL, Lang K, Meenan NA, Sharma A, Kelley AC, Kleanthous C, Ramakrishnan V. Structural basis for 16S ribosomal RNA cleavage by the cytotoxic domain of colicin E3. Nat Struct Mol Biol. 2010; 17:1241–1246. [PubMed: 20852642]

Nikolakakis K, Amber S, Wilbur JS, Diner EJ, Aoki SK, Poole SJ, Tuanyok A, Keim PS, Peacock S, Hayes CS, et al. The toxin/immunity network of *Burkholderia pseudomallei* contact-dependent growth inhibition (CDI) systems. Mol Microbiol. 2012; 84:516–529. [PubMed: 22435733]

Ogawa T, Tomita K, Ueda T, Watanabe K, Uozumi T, Masaki H. A cytotoxic ribonuclease targeting specific transfer RNA anticodons. Science. 1999; 283:2097–2100. [PubMed: 10092236]

Perez A, Canle D, Latasa C, Poza M, Beceiro A, Tomas Mdel M, Fernandez A, Mallo S, Perez S, Molina F, et al. Cloning, nucleotide sequencing, and analysis of the AcrAB-TolC efflux pump of *Enterobacter cloacae* and determination of its involvement in antibiotic resistance in a clinical isolate. Antimicrob Agents Chemother. 2007; 51:3247–3253. [PubMed: 17638702]

Pingoud A, Jeltsch A. Structure and function of type II restriction endonucleases. Nucleic Acids Res. 2001; 29:3705–3727. [PubMed: 11557805]

Poole SJ, Diner EJ, Aoki SK, Braaten BA, t'Kint de Roodenbeke C, Low DA, Hayes CS. Identification of functional toxin/immunity genes linked to contact-dependent growth inhibition (CDI) and rearrangement hotspot (Rhs) systems. PLoS Genet. 2011; 7:e1002217. [PubMed: 21829394]

Richardson RM, Pares X, Cuchillo CM. Chemical modification by pyridoxal 5'-phosphate and cyclohexane-1,2-dione indicates that Lys-7 and Arg-10 are involved in the p2 phosphate-binding subsite of bovine pancreatic ribonuclease A. Biochem J. 1990; 267:593–599. [PubMed: 2111131]

Riley MA. Positive selection for colicin diversity in bacteria. Mol Biol Evol. 1993; 10:1048–1059. [PubMed: 8412648]

Riley MA, Gordon DM. A survey of Col plasmids in natural isolates of *Escherichia coli* and an investigation into the stability of Col-plasmid lineages. J Gen Microbiol. 1992; 138:1345–1352. [PubMed: 1512564]

Rojas CM, Ham JH, Deng WL, Doyle JJ, Collmer A. HecA, a member of a class of adhesins produced by diverse pathogenic bacteria, contributes to the attachment, aggregation, epidermal cell killing, and virulence phenotypes of *Erwinia chrysanthemi* EC16 on *Nicotiana clevelandii* seedlings. Proc Natl Acad Sci U S A. 2002; 99:13142–13147. [PubMed: 12271135]

Rojas CM, Ham JH, Schechter LM, Kim JF, Beer SV, Collmer A. The *Erwinia chrysanthemi* EC16 *hrp/hrc* gene cluster encodes an active Hrp type III secretion system that is flanked by virulence genes functionally unrelated to the Hrp system. Mol Plant Microbe Interact. 2004; 17:644–653. [PubMed: 15195947]

Ruhe ZC, Low DA, Hayes CS. Bacterial contact-dependent growth inhibition. Trends Microbiol. 2013a; 21:230–237. [PubMed: 23473845]

Ruhe ZC, Wallace AB, Low DA, Hayes CS. Receptor polymorphism restricts contact-dependent growth inhibition to members of the same species. mBio. 2013b; 4:e00480–e00413. [PubMed: 23882017]

Schaller K, Nomura M. Colicin E2 is DNA endonuclease. Proc Natl Acad Sci U S A. 1976; 73:3989–3993. [PubMed: 1069283]

Senior BW, Holland IB. Effect of colicin E3 upon the 30S ribosomal subunit of *Escherichia coli*. Proc Natl Acad Sci U S A. 1971; 68:959–963. [PubMed: 4930243]

Silverman JM, Brunet YR, Cascales E, Mougous JD. Structure and regulation of the type VI secretion system. Annu Rev Microbiol. 2012; 66:453–472. [PubMed: 22746332]

Soelaiman S, Jakes K, Wu N, Li C, Shoham M. Crystal structure of colicin E3: implications for cell entry and ribosome inactivation. Mol Cell. 2001; 8:1053–1062. [PubMed: 11741540]

Tan Y, Riley MA. Positive selection and recombination: major molecular mechanisms in colicin diversification. Trends Ecol Evol. 1997; 12:348–351. [PubMed: 21238101]

Walker D, Lancaster L, James R, Kleanthous C. Identification of the catalytic motif of the microbial ribosome inactivating cytotoxin colicin E3. Protein Sci. 2004; 13:1603–1611. [PubMed: 15133158]

Webb JS, Nikolakakis KC, Willett JL, Aoki SK, Hayes CS, Low DA. Delivery of CdiA nuclease toxins into target cells during contact-dependent growth inhibition. PLoS ONE. 2013; 8:e57609. [PubMed: 23469034]

Zhang D, de Souza RF, Anantharaman V, Iyer LM, Aravind L. Polymorphic toxin systems: Comprehensive characterization of trafficking modes, processing, mechanisms of action, immunity and ecology using comparative genomics. Biol Direct. 2012; 7:18. [PubMed: 22731697]

Zhang D, Iyer LM, Aravind L. A novel immunity system for bacterial nucleic acid degrading toxins and its recruitment in various eukaryotic and DNA viral systems. Nucleic Acids Res. 2011; 39:4532–4552. [PubMed: 21306995]

Zheng J, Ho B, Mekalanos JJ. Genetic analysis of anti-amoebae and anti-bacterial activities of the type VI secretion system in *Vibrio cholerae*. PLoS ONE. 2011; 6:e23876. [PubMed: 21909372]

Highlights

- Contact-dependent growth inhibition (CDI) systems mediate inter-bacterial competition.
- We present the structure of the *Enterobacter cloacae* CDI^{ECL} toxin/immunity complex.
- The CDI^{ECL} toxin displays a similar fold and nuclease activity as colicin E3.
- The structural similarities between these toxins likely reflect convergent evolution.

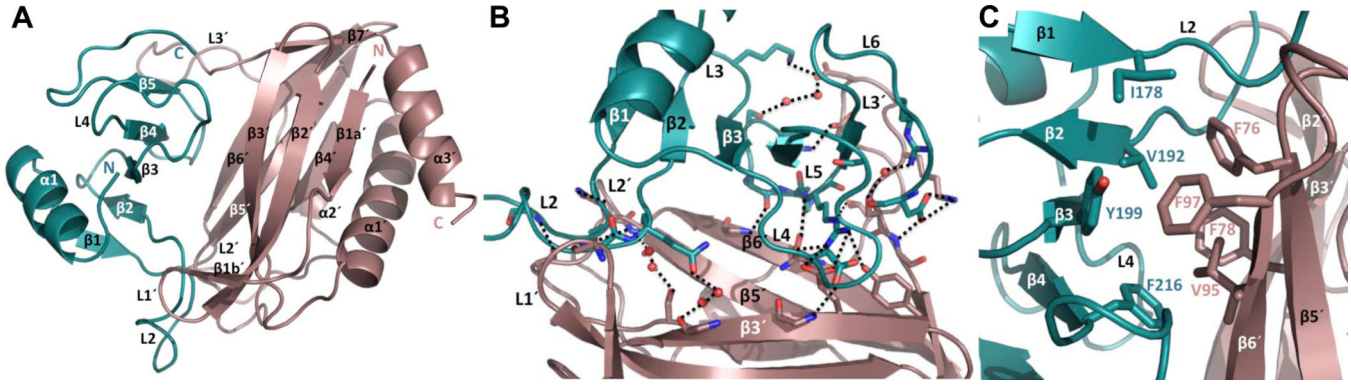

Figure 1. Structure of the CdiA-CT/CdiI^{ECL} complex

A) The CdiA-CT^{ECL} toxin (teal) and CdiI^{ECL} immunity protein (salmon pink) are depicted in ribbon representation with secondary structure elements. The amino and carboxyl termini are indicated by **N** and **C**, respectively. CdiI^{ECL} elements are denoted with a prime symbol (´) to differentiate them from the toxin secondary structure elements. **B**) The CdiA-CT/CdiI^{ECL} interface is mediated by an extensive network of ion-pair and hydrogen-bond interactions. Water molecules are depicted as red spheres and interacting bonds as black dotted lines. **C**) The CdiA-CT/CdiI^{ECL} interface also contains hydrophobic interactions mediated by the residues indicated in one-letter code. The view in panel B represents a 90° clockwise rotation of panels A & C. Also see Fig. S1.

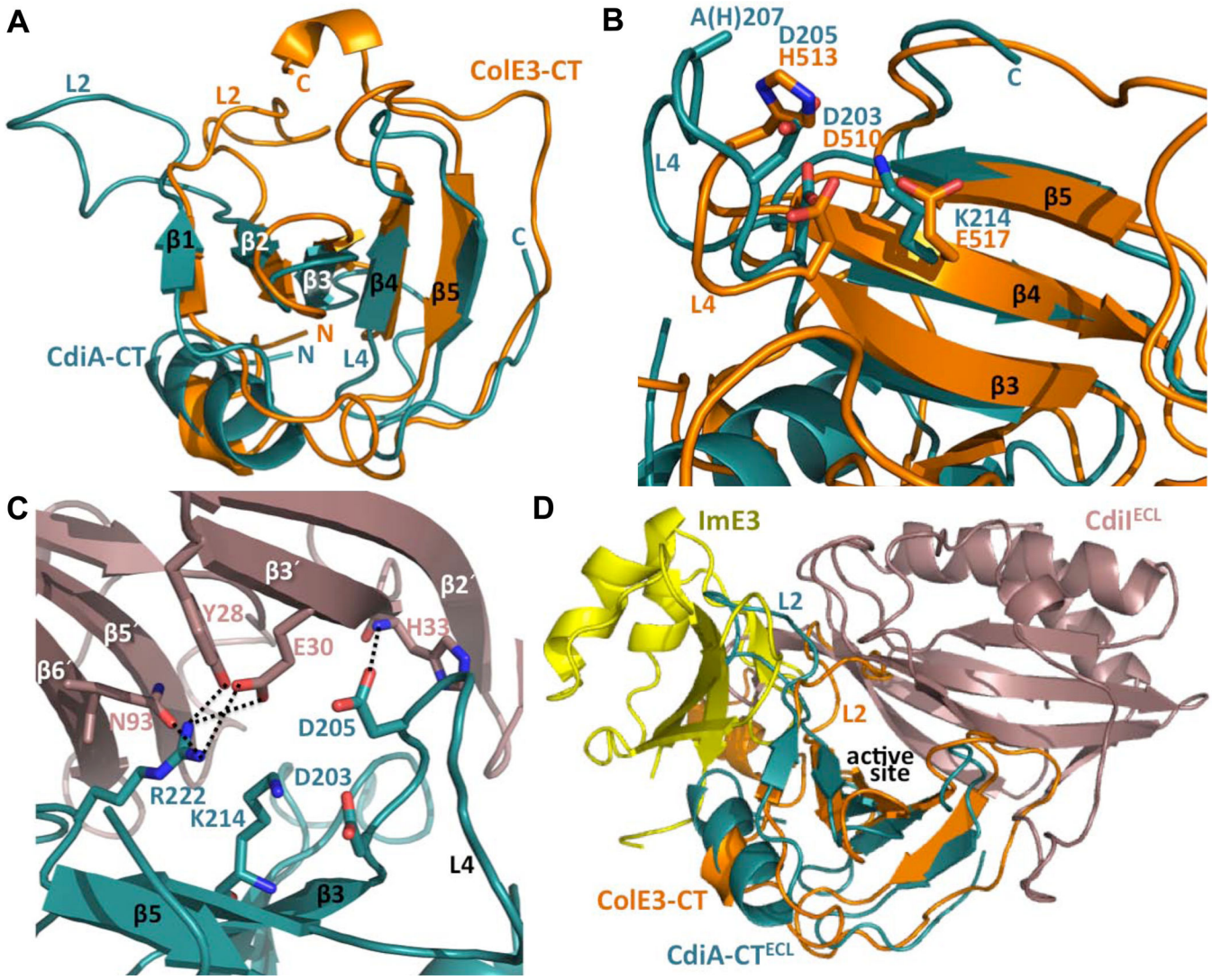

Figure 2. CdiA-CT^{ECL} share structural similarities with the nuclease domain of colicin E3

A) Superimposition of CdiA-CT^{ECL} (teal) and the C-terminal nuclease domain of colicin E3 (ColE3-CT, orange) (PDB ID: 2B5U). The toxin domains superimpose with an rmsd of 2.1 Å. **B**) Colicin E3 residues Asp510, His513 and E517 are involved in catalysis and superimpose with residues Asp203, Asp205 and Lys214 of CdiA-CT^{ECL}. His207 of CdiA-CT^{ECL} is located within disordered loop L4 and is modeled as an alanine residue. Residues are indicated in one-letter code and rendered as stick representations. **C**) The predicted CdiA-CT^{ECL} active site is occluded by bound CdiI^{ECL}. Interacting bonds are represented by black dotted lines. **D**) Superimposition of CdiA-CT/CdiI^{ECL} with the ColE3-CT/ImE3 complex. Ribbon representations of CdiA-CT^{ECL} (teal), CdiI^{ECL} (salmon pink), ColE3-CT (orange) and ImE3 (yellow) are depicted. Also see Figs. S2 and S3.

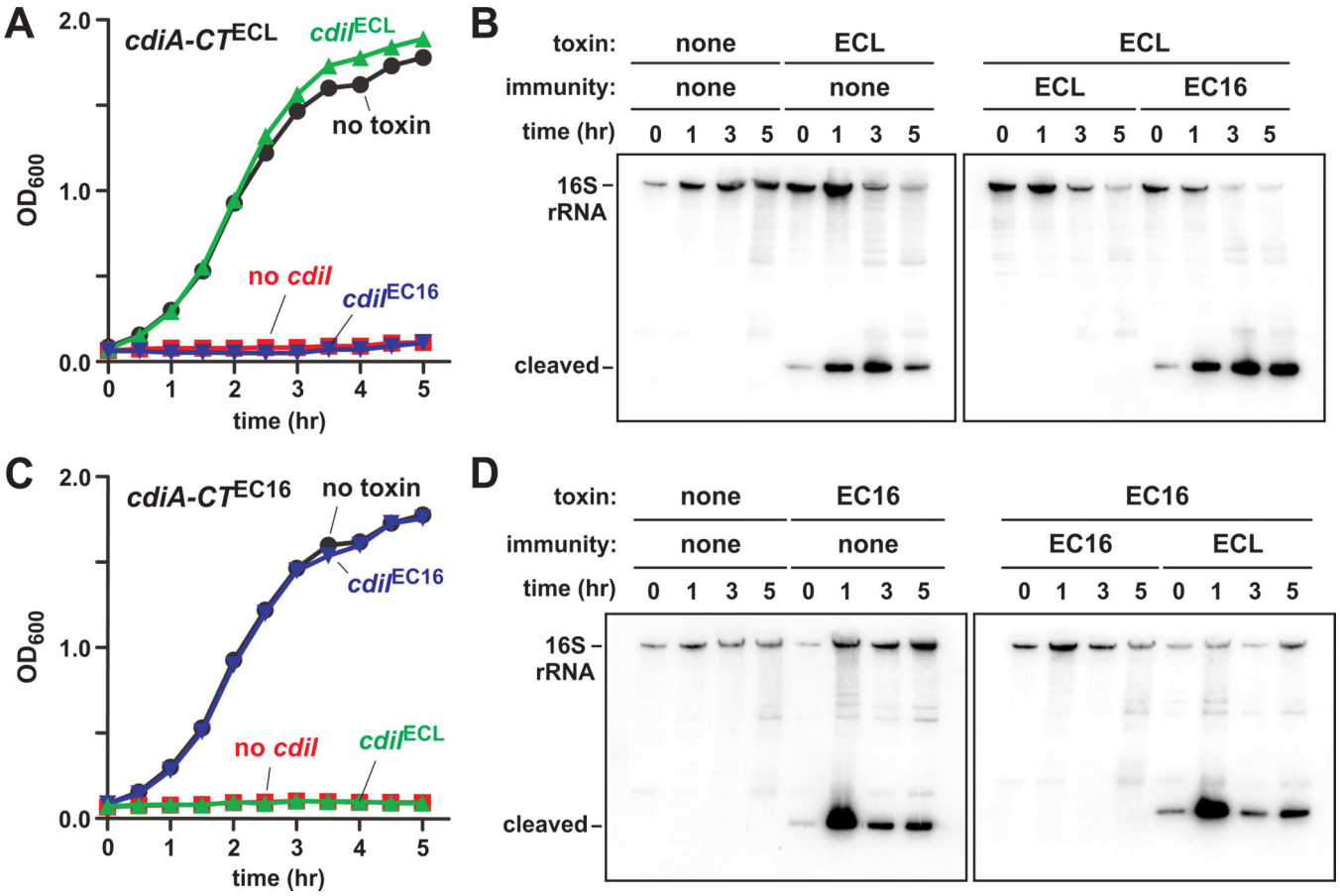

Figure 3. CdiA-CT toxin activity *in vivo*

A & **C**) Toxin expression was induced at 0 hr and cell growth monitored by measuring the culture optical density at 600 nm (OD_{600}). Red curves are from cells that lack an immunity gene; and the green and blue curves represent cells that express *cdiI*^{ECL} and *cdiI*^{EC16}, respectively. The black curve shows cell growth in the absence of toxin expression. **B** & **D**) Total RNA was isolated from the cells in panels A & C and analyzed by northern blot using a probe to the 3´-end of *E. coli* 16S rRNA. Toxin and immunity genes are indicated as **ECL** for *E. cloacae* and **EC16** for *E. chrysanthemi* EC16. The migration positions of full-length and cleaved 16S rRNA are indicated. Also see Fig. S4.

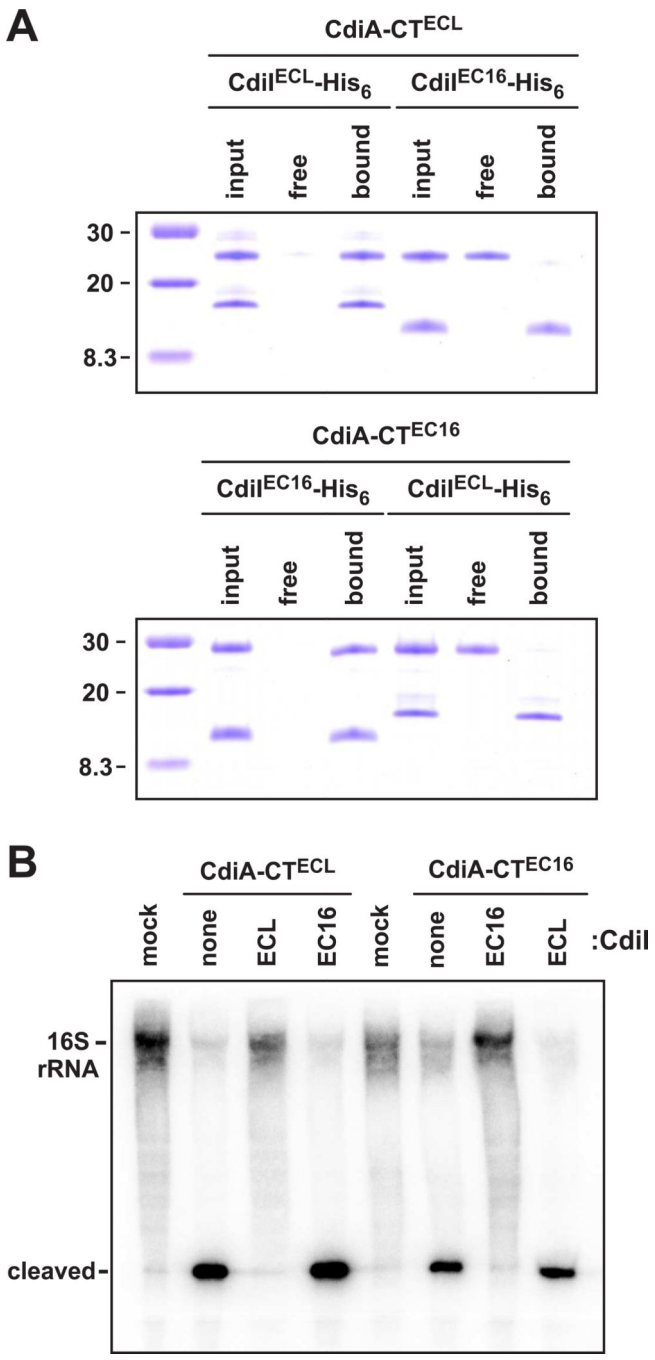

Figure 4. CdiA-CT toxin activity *in vitro*

A) Purified CdiA-CT toxins and CdiI-His_6 immunity proteins were mixed, then subjected to Ni^{2+}-affinity chromatography under non-denaturing conditions. Lanes labeled **input** represent CdiA-CT/CdiI-His_6 mixtures prior to chromatography, lanes labeled **free** are proteins that fail to bind Ni^{2+}-resin, and lanes labeled **bound** are proteins that elute with imidazole. **B**) Isolated *E. coli* ribosomes were treated with purified CdiA-CT^{ECL} and CdiA-CT^{EC16}, and the reactions analyzed by northern blot using a probe to the 3′-end of 16S rRNA. Where indicated, CdiI-His_6^{ECL} (**ECL**) or CdiI-His_6^{EC16} (**EC16**) was added at an

equimolar ratio to the toxin. Mock reactions are ribosome samples that were treated with buffer. The migration positions of full-length and cleaved 16S rRNA are indicated.

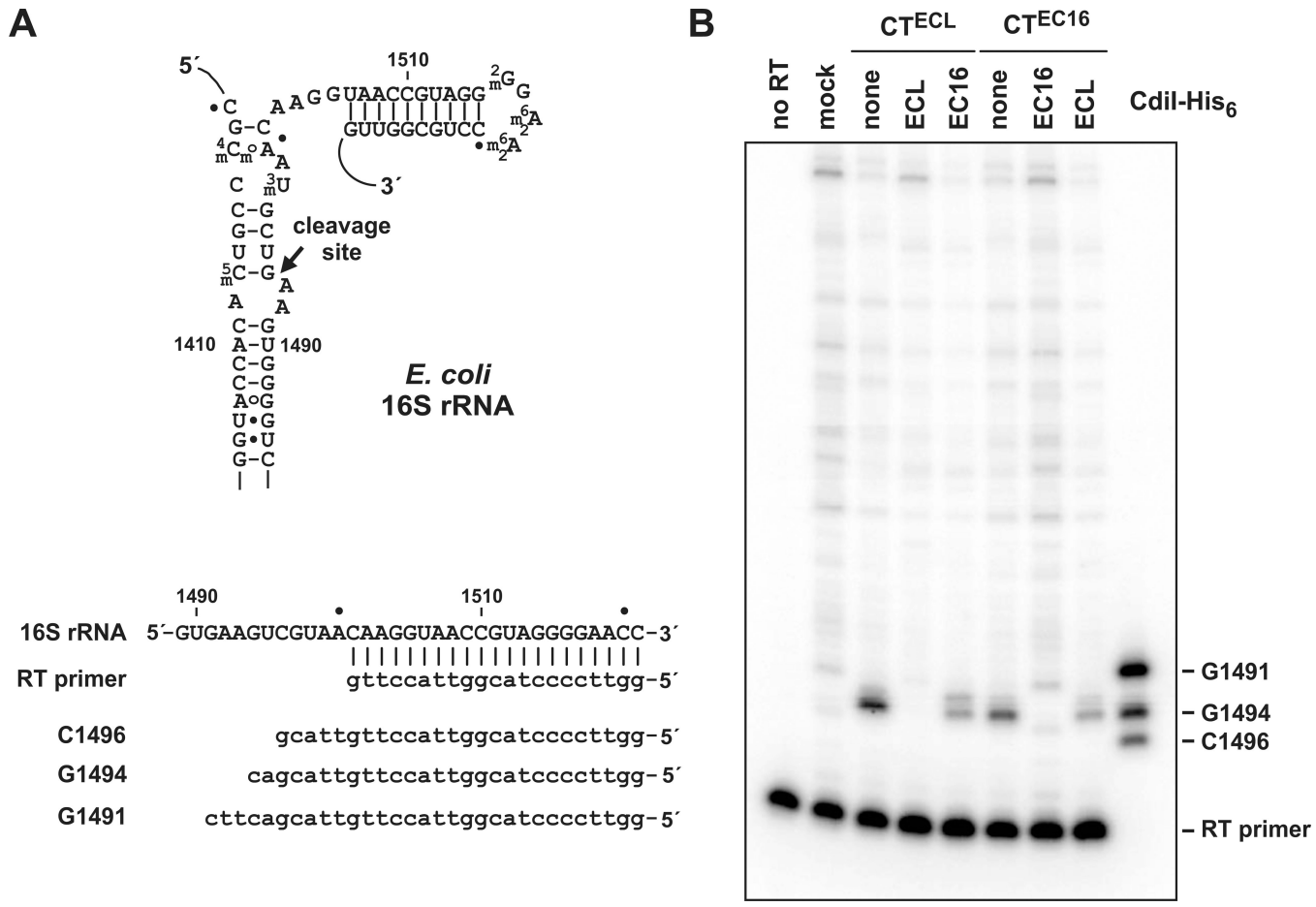

Figure 5. CdiA-CT^{ECL} and CdiA-CT^{EC16} cleave 16S rRNA between A1393 and G1394

A) Nucleotide sequence and secondary structure of the 30S subunit decoding center. The sequence of the reverse transcription (**RT**) primer is shown in heteroduplex with its complementary sequence in 16S rRNA. Oligonucleotides **C1496**, **G1494** and **G1491** were used as gel-migration standards. The 16S rRNA cleavage site is indicated by an arrow. **B**) Ribosomal RNA was extracted from the indicated *in vitro* nuclease reactions and hybridized to radiolabeled **RT primer** for primer extension analysis using reverse transcriptase. Reactions were resolved on a denaturing gel and visualized by phosphorimaging. The migration positions of oligonucleotides **C1496**, **G1494** and **G1491** are indicated.

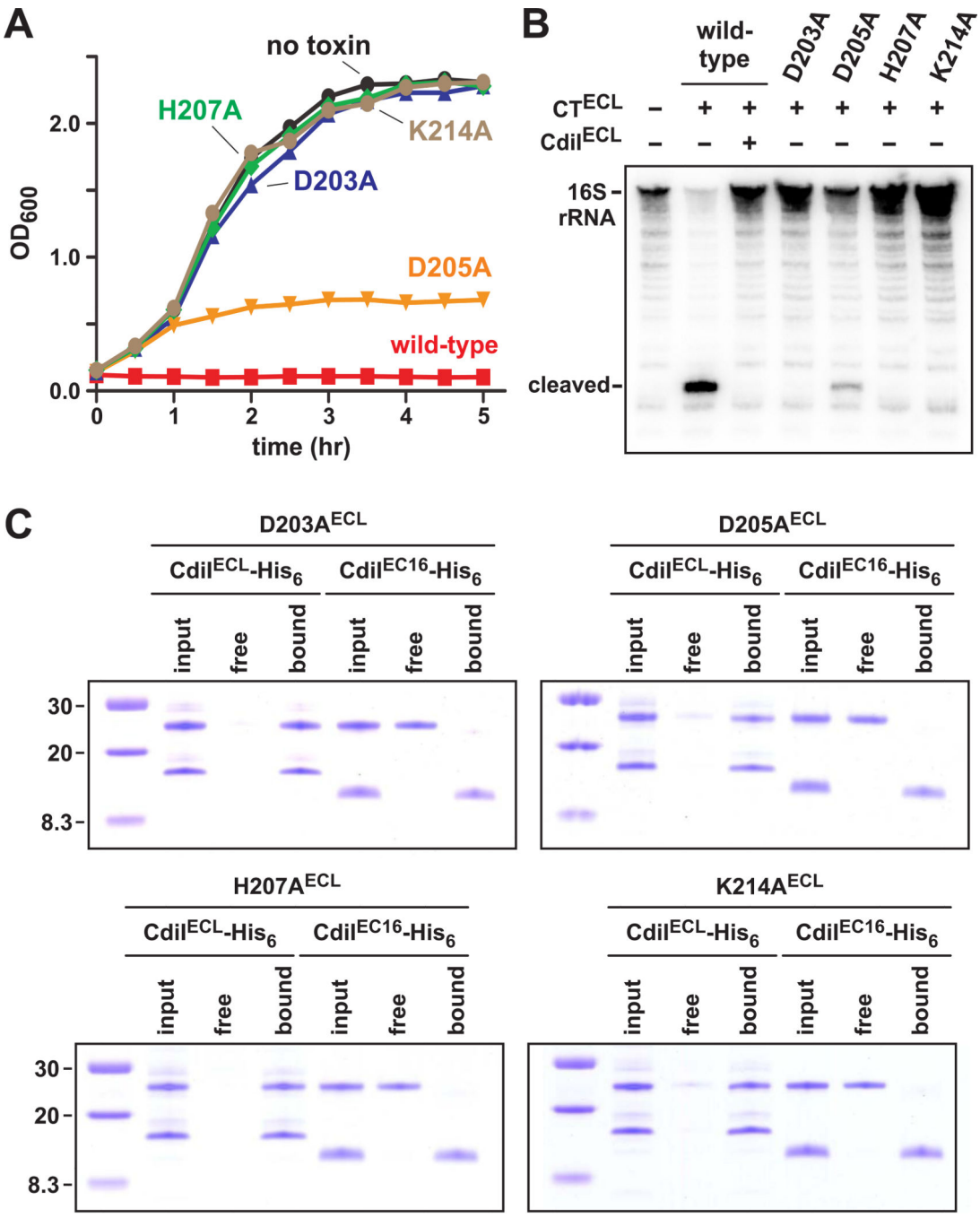

Figure 6. Mutagenesis of predicted active-site residues in CdiA-CT^{ECL}

A) Expression of *cdiA-CT*^{ECL} and the indicated mutated variants were induced at 0 hr with L-arabinose and cell growth monitored by measuring the optical density of the culture at 600 nm (OD_{600}). The black curve shows the growth of a control culture without toxin expression. **B**) Isolated *E. coli* ribosomes were treated with purified CdiA-CT^{ECL} toxins and RNA extracted for northern blot analysis. Where indicated, purified CdiI-His_6^{ECL} was included in the reaction. The gel-migration positions of full-length and cleaved 16S rRNA are indicated. **C**) Purified CdiA-CT toxins and CdiI-His_6 immunity proteins were mixed,

then subjected to Ni^{2+}-affinity chromatography under non-denaturing conditions. Lanes labeled **input** represent CdiA-CT/CdiI-His_6 mixtures prior to chromatography, lanes labeled **free** are proteins that fail to bind Ni^{2+}-resin, and lanes labeled **bound** are proteins that elute with imidazole.

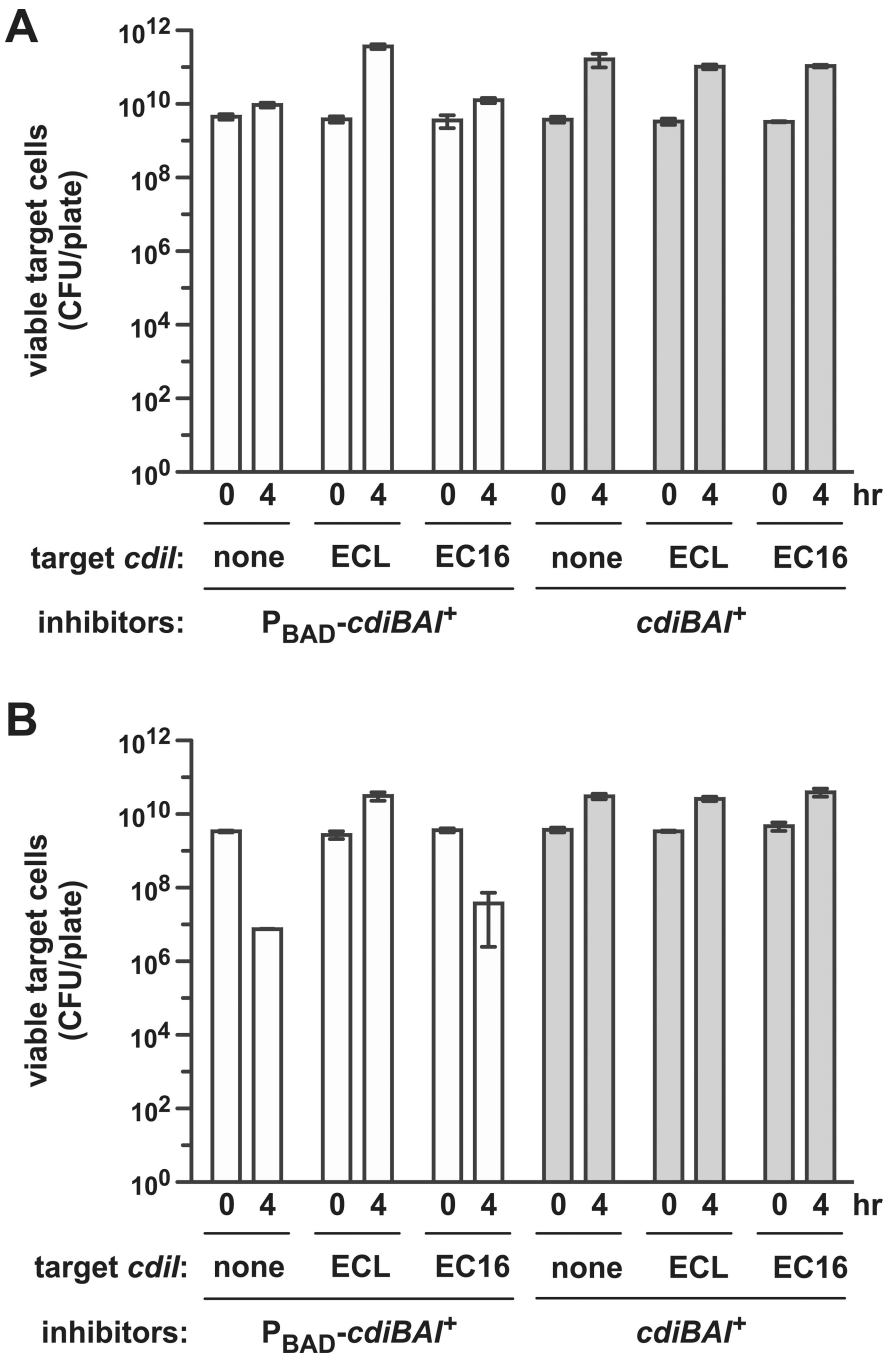

Figure 7. Intercellular competitions with *E. cloacae* inhibitor cells

A) Intra-species competition. *E. cloacae* inhibitor cells were co-cultured with *E. cloacae* Δ*cdiA*^{ECL} Δ*cdiI*^{ECL} target cells on LB-agar supplemented with arabinose. Where indicated, target cells were provided with plasmid-borne *cdiI*^{ECL} or *cdiI*^{EC16} immunity genes. Total viable target cells were determined as colony forming units. White bars correspond to competitions with arabinose-inducible inhibitor cells (P_{BAD}-*cdiBAI*$^{+}$), and grey bars correspond to competitions with inhibitors that carry the wild-type locus (*cdiBAI*$^{+}$). **B**) Inter-species competition. *E. cloacae* inhibitor cells were co-cultured with *E. coli* target cells on

LB-agar supplemented with arabinose. Where indicated, the target cells were provided with plasmid-borne *cdiI*^{ECL} or *cdiI*^{EC16} immunity genes. Viable target cells were determined as colony forming units (CFU), and data are reported as the mean ± SEM for two independent experiments.

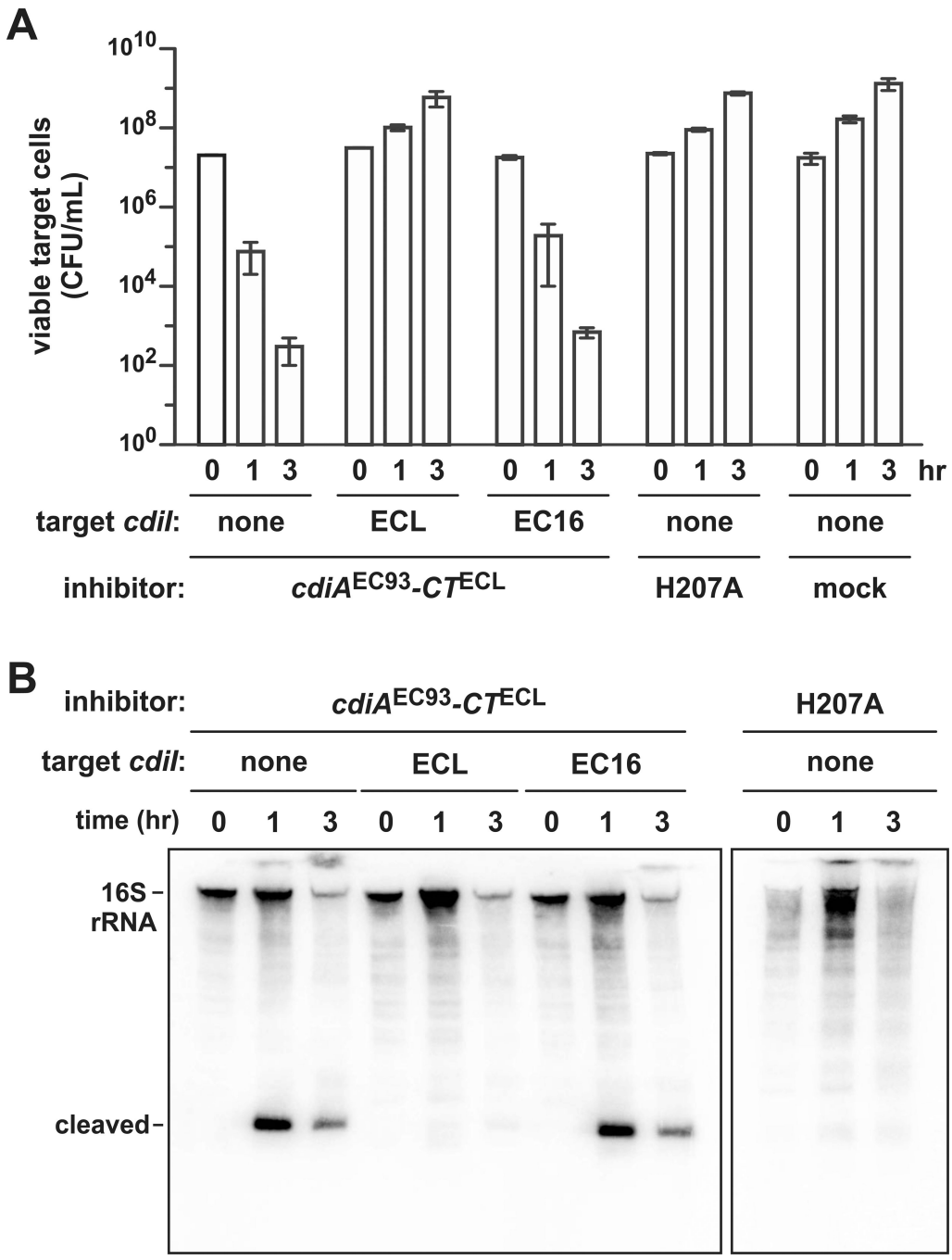

Figure 8. The CdiA-CT^{ECL} toxin domain is modular

A) *E. coli* target cells were co-cultured with inhibitor cells that express chimeric CdiA^{EC93}-CT^{ECL} in broth. Where indicated, target cells were provided with plasmid-borne copies of the *cdiI*^{ECL} or *cdiI*^{EC16} immunity genes. The inhibitors labeled **H207A** express CdiA^{EC93}-CT^{ECL} containing the His207Ala mutation in the toxin domain. Mock inhibitors lack the CDI system. Viable target cell counts were determined as CFU/mL, and data are reported as the mean ± SEM for two independent experiments. **B**) Total RNA was isolated from the co-

culture experiments described in panel A and analyzed by northern blot using a probe to the 3′-end of 16S rRNA.

Table 1

Crystallographic statistics for the CdiA-CT^{ECL}/CdiI^{ECL} protein complex

	Peak	Remote	Inflection	Native
Space Group	$P4_122$	$P4_122$	$P4_122$	$P4_122$
Unit cell dimensions (Å)	85.64 85.64 75.17	85.64 85.64 75.17	85.64 85.64 75.17	85.25 85.25 74.91
pH of crystallization condition	5.1	5.1	5.1	5.1
Protein concentration (mg/mL)		9	9	9
Data set	9			
Wavelength (Å)	0.9759	1.377	0.9794	1
Resolution range	50–2.85	50–3.0	50–2.9	50–2.4
Unique reflections (total)	5486 (191798)	4645 (163018)	5179 (181470)	11315 (324387)
Completeness (%)*	100.0 (100.0)	100.0 (100)	100.0 (100.0)	100 (100)
Redundancy *	27.8 (28.8)	27.6 (28.5)	27.8 (28.7)	28.7 (29.3)
R_{merge} *,†	0.114 (0.47)	0.129 (0.501)	0.109 (0.445)	0.088 (0.455)
I/σ*	31.1 (10.42)	27.8 (8.7)	34.8 (10.8)	44.7 (11)
NCS copies	1			1
No. of Selenium sites/a.u	6			
FOM	0.49			
Model refinement				
Resolution range (Å)				38.125-2.400
No. of reflections (working/free)				11291/538
No. of protein atoms				1760
No. of water molecules				62
Missing residues				CdiA-CT 1–160
R_{work}/R_{free} ‡, %				23.7/18.3
R.m.s deviations				
Bond lengths (Å)				0.008
Bond angles (degrees)				1.15
Ramachandran Plot				
Most favorable region (%)				93.61
Additional allowed region (%)				6.39
Disallowed region				0.0
PDB ID Code				4NTQ

* Statistics for the highest resolution shell are given in (brackets)

† $R_{merge}=\Sigma|I-<I>|/\Sigma I$

‡ $R_{work}=\Sigma|F_{obs}-F_{calc}|/\Sigma F_{obs}$ R_{free} was computed identically except where all reflections belong to a test set of 10% randomly selected data.